Potassium permeation through the KcsA channel: a density functional study

Leonardo Guidoni[1], Paolo Carloni [*]

Istituto Nazionale per la Fisica della Materia (INFM), Italy and International School for Advanced Studies (SISSA), Via Beirut 4, 34014 Trieste, Italy

Abstract

We present a theoretical study on structural and electronic aspects of K^+ permeation through the binding sites of the KcsA channel's selectivity filter. Density functional calculations are carried out on models taken from selected snapshots of a molecular dynamics simulation recently reported [FEBS Lett. 477 (2000) 37]. During the translocation process from one binding site to the other, the coordination number of the permeating K^+ ion turns out to decrease and K^+ ion polarizes significantly its ligands, backbone carbonyl groups and a water molecule. K^+-induced polarization increases significantly at the transition state (TS) between the two binding sites. These findings suggest that polarization effects play a significant role in the microscopic mechanisms regulating potassium permeation. © 2002 Elsevier Science B.V. All rights reserved.

1. Introduction

Potassium channels are membrane proteins regulating a vast variety of biophysical processes [1,2]. The channels can select permeation of K^+ ions against anions (such as Cl^-), multivalent cations (such as Ca^{2+}), and against alkali ions other than K^+ (such as Na^+).

The recently determined X-ray structure of the KcsA potassium channel from *Streptomyces lividans* (Fig. 1A) has individuated the machinery responsible for ion selectivity and permeation [3]. This is the so-called 'selectivity filter', a narrow pore formed by highly conserved residues (TVGYG) (Fig. 1B). The filter has four binding sites, which can be occupied by monovalent cations or water molecules (S1–S4 in Fig. 1B). In binding sites S1–S3, Thr75–Tyr78 carbonyls of the four subunits bind to the metal ion. The resulting coordination is eight. In binding site S4, the same coordination is found, but Thr75 side chain also participates to the binding. The two lower binding sites (S3–S4) are not simultaneously occupied by ions [3,4].

Force-field molecular dynamics simulations studies have identified spontaneous [5–8] and activated [9–11] path-ways through the selectivity filter of varying complexity, involving different number of loading states. Furthermore, they have shown that permeation occurs through a 'single-file' translocation (backward or inward) of ions and water molecules into the selectivity filter.

In this paper, we address fundamental issues related to the reliability of methodology. The first point concerns the transferability of K^+ force field. This has been parameterized for simulations in water [12–14], and therefore it may find difficulties in describing metal/protein interactions, and, more, in the calculation of energetics associated to translocation process, which is essentially a ligand-exchange chemical reaction in a metal complex [15]. Further problems may lie on the neglect of polarization effects, which have already been shown to be of importance in several molecular recognition processes [16–18]. These effects are more reliably described by ab initio quantum chemical methods.

In an attempt at understanding the role of the electronic structure for potassium permeation, we have here undertaken a first principles Density Functional Theory (DFT) calculations. The DFT approach allows us to handle relatively large systems at a moderate computational cost and can be extended in the future to dynamical studies in the framework of Car-Parrinello Molecular Dynamics [19] and hybrid CPMD/MM calculations [20].

Our investigation is carried out in two steps. First, we analyze the coordination chemistry and the ligand geometry

---

[*] Corresponding author. Tel.: +39-40-3787-407; fax: +39-40-3787-528.
E-mail address: carloni@sissa.it (P. Carloni).
[1] Present address: Institute of Inorganic Chemistry ETH Zürich, HCI-Hönggerberg, 8093 Zürich, Switzerland.
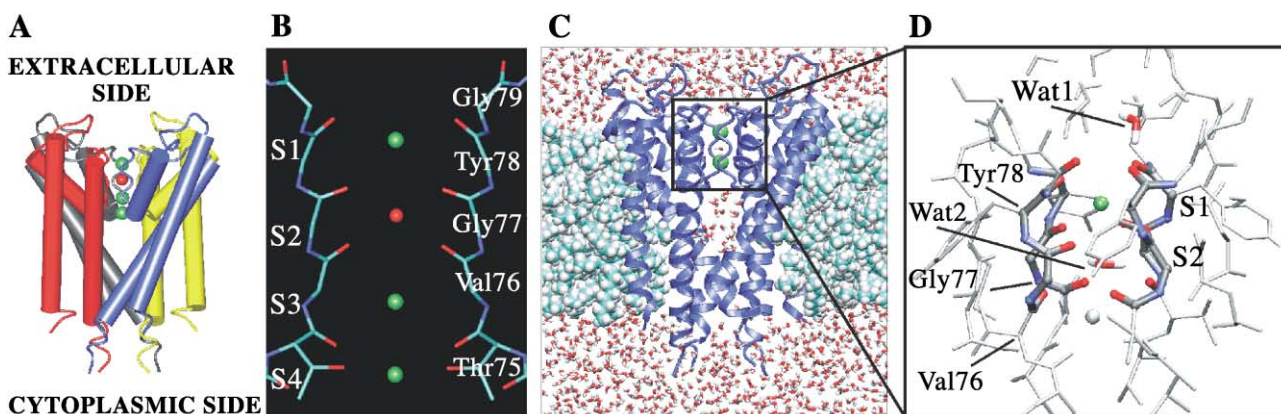
Fig. 1. Structure of the KcsA K$^+$ channels [3]. (A) The protein is a tetramer; each monomer contains two transmembrane helices forming the pore across the cell membrane through which ions may flow. (B) The selectivity filter is constituted by Thr75–Gly79 backbone atoms. Four binding sites (S1–S4) were identified by X-ray [3] for K$^+$ ions (green spheres) and a water molecule (red sphere). Backbone and Thr75 heavy atoms belonging two of the four subunits are represented by sticks. (C) Molecular model used in the molecular dynamics (MD) calculations [8]. The protein (blue ribbons) with two K$^+$ ions (green spheres) in its selectivity filter was immersed in a water/n-octane bilayer. (D) Close up on the selectivity filter. The quantum-mechanical model used in the calculations is highlighted. Protein hydrogen atoms are not shown for clarity.

changes of the ion translocation observed in a recent classical MD simulation [8]. Second, we carry out the DFT study of models based on selected snapshots from the MD, following the procedure successfully used to address a similar issue in gramicidin [21] and in other systems [22].

2. Material and methods

2.1. Structural analysis

The analysis of the K$^+$ coordination was based on our recent MD simulation of the KcsA potassium channel with two K$^+$ ions inside the selectivity filter (model 2K of Ref. [8]) (Fig. 1C). In this paper, we showed that the ionic positions S1 and S3 are stable on nanosecond time scale only if one additional ion is present into the internal cavity of the channel [8]. Indeed, the two-ion simulation 2K leaded in ~100 ps to a single-file movement of one binding site towards the intracellular direction.

2.2. Quantum chemistry calculations

Analysis of the electronic structure of MD snapshots can be carried out by performing single point calculations on conformations generated by classical MD simulations [21,22]. Here, we extracted atomic positions from the previously described MD simulation of model 2K [8]. The simulation was based on the X-ray structure from Doyle et al. [3] (Protein Data Bank accession number 1BL8) and it was performed using an n-octane slab to mimic the membrane environment. At present, it is not possible to calculate the electronic structure of the entire protein with first-principles methods. Therefore, we considered here a cluster model that appears to capture the local K$^+$/protein inter-

action (Fig. 1D). The model includes: (i) the group forming binding sites S1 and S2, namely the backbone segment from C(Val76) to N(Gly79) of each subunit; (ii) the K$^+$ ion in the state S1; (iii) water molecules Wat2 (already detected in the X-ray structure) and Wat1 (present in the MD simulation [8]). The C$_\alpha$ and backbone termini were saturated by hydrogen atoms. This model is expected to provide a reasonable description of protein/K$^+$ interactions. Hydrogen atoms were added assuming standard bond lengths and bond angles. The total charge of the model complex is +1. Using the simple electrostatic calculation of Ref. [23], we verified that the electrostatic fields experienced on the potassium ion and its ligand oxygens in our model differ at most by 30% those into the full KcsA model [8].

Eleven snapshots of the MD simulation at room temperature were collected in the 60 ps time window. In this timescale, the ions moved from one site to another (Fig. 2A). As initial configuration (frame f0), we took the snapshot after 96 ps of dynamics 2K [8]. The subsequent frames f1–f10 were collected every 5.7 ps. The figure shows that during this relatively short dynamics, a translocation of the K$^+$ ion from site S1 to S2 occurs. We expect that our results do not qualitatively change upon geometry optimization.

2.3. Computational details

The computational details of the MD simulation are reported in Ref. [8]. We solved the quantum problem with DFT [24], in the formulation by Kohn and Sham [25], using the local density approximation with BLYP gradient correction [26,27]. The core–valence electron interaction was described using Martins and Troullier pseudopotentials [28]. The systems were treated as isolated [29]. The Kohn and Sham orbitals were expanded in a plane wave basis set up to an energy cutoff of 70 Ry. The electronic wave function was optimized up to a gradient less than 5×10^{-7} a.u.
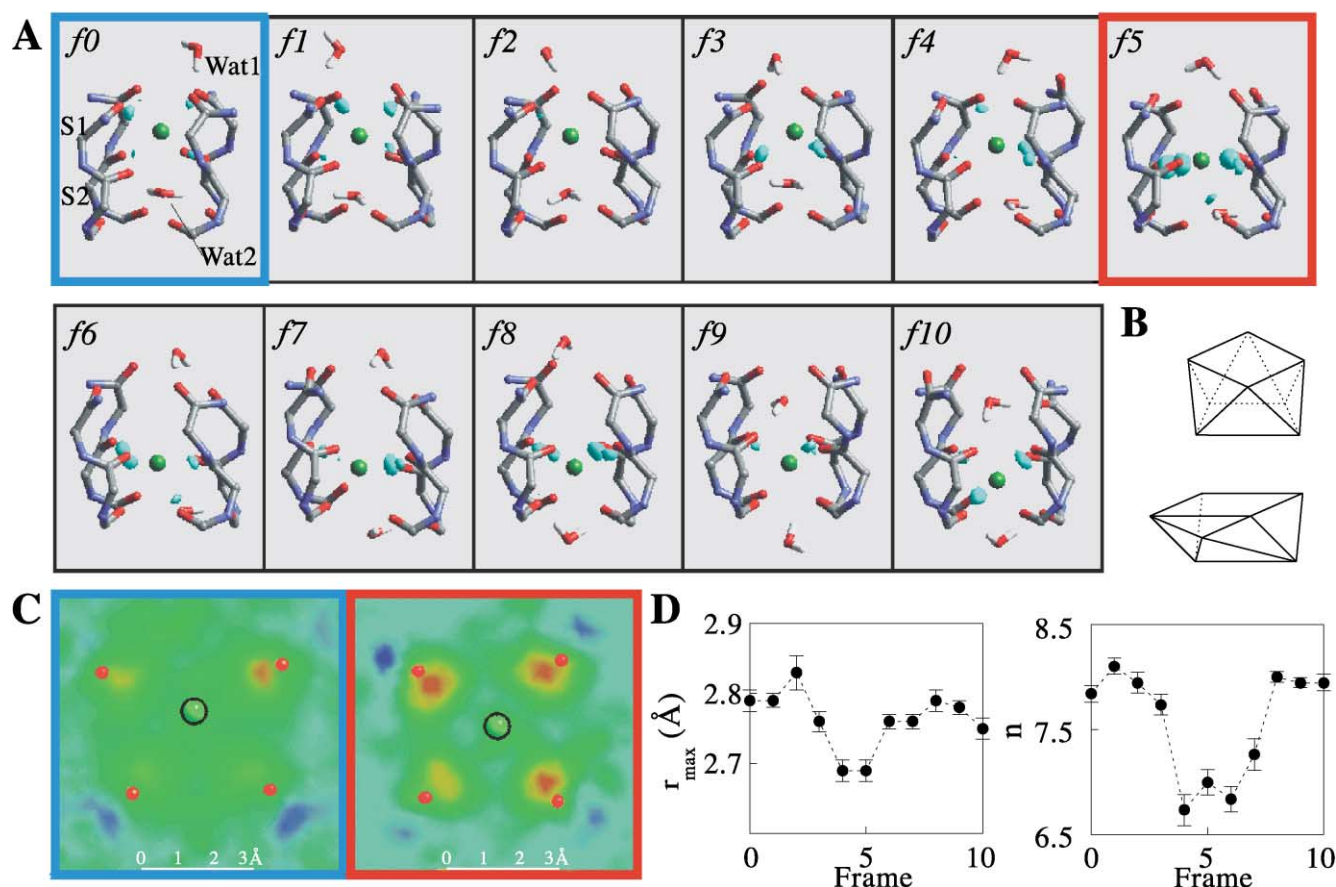
Fig. 2. K^+ permeation through the selectivity filter. (A) Eleven snapshots f0–f10 (each taken 5.7 ps of dynamics) from the classical MD simulation [8]. The difference electron density $\Delta\rho$ is superimposed to the molecular structure in light blue color (the contour level 0.0202 e/Å^3). (B) Geometry of the potassium coordination polyhedra. At the binding site (frame f0), the metal ion is eight-coordinated with antiprismatic geometry (upper sketch). At the TS (frame f5), only seven ligands bind to the K^+ and the geometry is pyramidate triangular prismatic (lower sketch). (C) $\Delta\rho$ of frames f0 and f5 is projected on a best-fit plane containing K^+ ion and the four donor atoms, which are mostly polarized (two Tyr78 oxygens and two Gly77 oxygens for frame f0, four Gly77 oxygens for frame f5). $\Delta\rho$ ranges from blue (-0.0135 e/Å^3) to red (0.0304 e/Å^3). (D) K^+ coordination. The position r_{max} of the maximum of the radial distribution function $g(r_{K^+-O})$ (left) and its integral (the coordination number n) is plotted as a function of the frames f0–f10.

2.4. Calculated properties

(i) Potassium–oxygen radial distribution functions $g(r_{K^+}-O)$ were calculated as in Ref. [30]. Their integration from zero to the first minimum in water ($r_{K^+}-O = 3.65$ Å [31]) provided an estimate of K^+ coordination number [2]. To have adequate statistics, the values of $g(r)$ for each frame f0–f1 (as reported in Figs. 2D and 3A) were obtained by averaging 190 MD snapshots within the 5.7 ps time windows around the frame. (ii) The electron density difference $\Delta\rho$ has been calculated by subtracting the densities of the metal ion and the ligands from the density of the complex: $\Delta\rho = \rho_{complex} - \rho_{ion} - \rho_{ligands}$. The charge difference ΔQ of

an atom was calculated as an integral of $\Delta\rho$ on a sphere centered on atom within a cutoff r_{cut}. The total rearranged charge Δq around an atom was calculated integrating the absolute value of $\Delta\rho$. (iii) The centers of the maximally localized Wannier orbitals were calculated as in Ref. [32].

3. Results

3.1. Structural features

Our previous classical MD simulation [8] showed that the two ions into the filter, initially located in S1 and S3 (Fig. 1B,D), spontaneously underwent a single-file movement shifting towards the intracellular direction in ≈ 60ps. Here we focus on the structural features of the translocation of K^+ from site S1 to site S2 (frames f0–f10 in Fig. 2A). The metal ion was bound to backbone carbonyls of the four subunits and to water molecules Wat1 and Wat2.

---

[2] In many MD snapshots (like in frames f8–f10), Wat2, although being within the K^+ first shell ligand cutoff, points its electric dipole towards the ion. This is caused by water hydrogen bonding to Val76 carbonylic oxygens. In these circumstances, the water molecule clearly does not bind the metal ion and it was excluded by the calculation of $g(r_{K^+-O})$.

In the initial configurations (f0, f1), the potassium ion was located in binding site S1 (Fig. 1B,D). The four Tyr78 and the four Gly77 backbone carbonyls were bonded to the metal ion in a distorted antiprismatic geometry (Fig. 2B, upper sketch). The K^+–O distance was large (Fig. 2D, left panel) and, as a consequence, the coordination number was

A

B

C
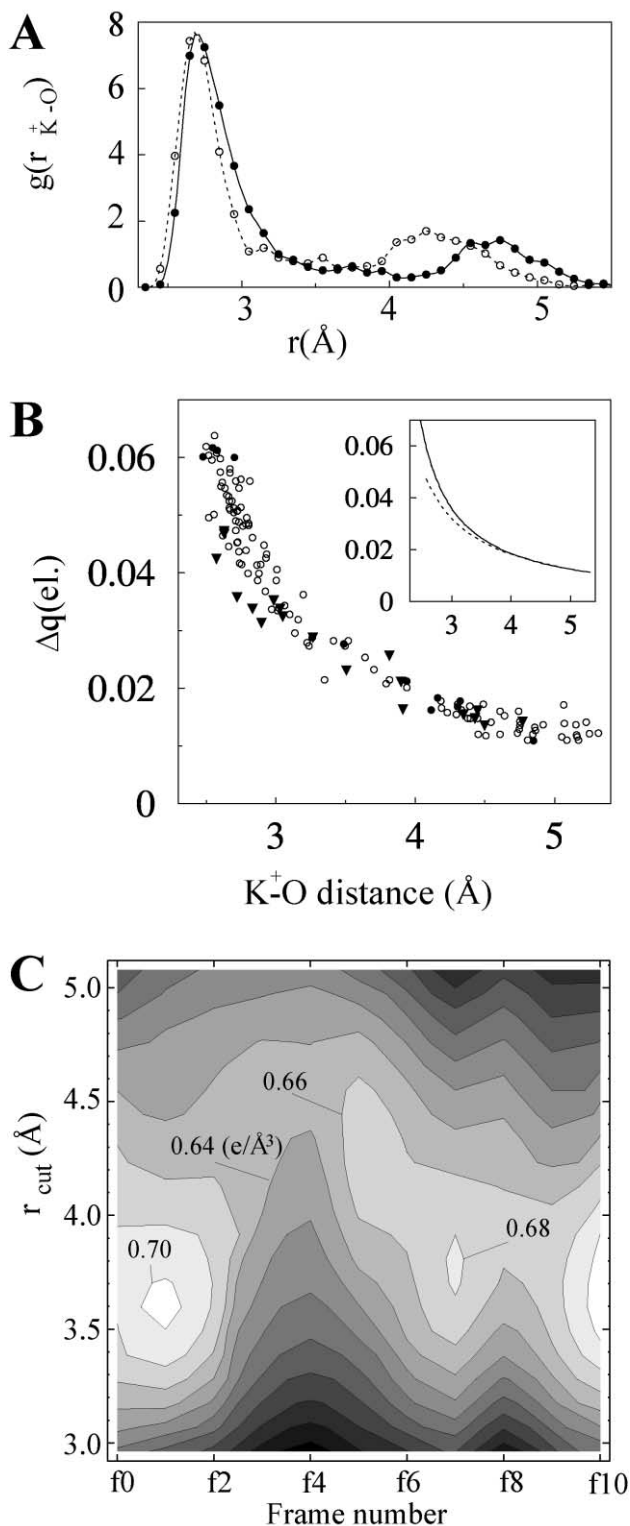
maximum (Fig. 2D, right panel). The interaction with second-shell ligands (Val76 and Wat1) was weak: it ranges from 4.4 to 5.3 Å.

In few picoseconds, the metal ion abandoned site S1 (frames f2–f4). In this process, it started losing its coordination with Tyr78 and it bound to Gly77 and Wat2. At the transition state (TS) (f5), it bound tightly to the four Gly77 and Wat2, and weakly to two backbone oxygens belonging to Val76 and Tyr78. The polyhedron geometry can be described as a highly distorted pyramidate triangular prism (Fig. 2B, lower sketch). K^+ coordination number and the K^+–O distances reached their minimum (Fig. 2D). As K^+ first-shell coordination number was smaller than in initial configurations, the interaction with the second-shell ligands (Val76 and Tyr78) became significant as evidenced by the second maximum of the radial distribution function (Fig. 3A).

Around the TS (frames f4–f7) Wat2 remained bound to K^+. In contrast, Wat1 did not participate to the ligand exchange process and it followed the ionic intracellular movement with some delay, leaving S1 unoccupied (frames f5–f8). Finally, the ion reached site S2 (f9–f10), previously occupied by Wat2, again characterized by a large coordination number. In S2, the ion bound exclusively to Gly77 and Val76, while both water molecules were H-bonded to carbonyls, without participating as ligands.

3.2. Polarization effects

The difference electron density $\Delta\rho$ describes the rearrangement of the electronic density upon K^+ binding to the protein. Polarization effects were clearly operative and involved the carbonyl oxygen donor atoms. Interestingly, the polarization effect induced by K^+ *increased on* passing from the binding site to TS (Fig. 2A,C). This is a consequence of the decrease of the K^+–O distance on passing from f0 to f5.

Fig. 3B shows that this is actually a general trend of the simulation. The charge rearrangement on ligand oxygens induced by the metal ion (Δq) is indeed correlated to the K^+–O distance: decreasing the metal–donor distance caused an increase of the polarization. Furthermore, polarization effects are still present at relatively large distances

Fig. 3. (A) Radial distribution function [$g(r_{K^+-O})$] for f0 (solid circles) and f4 (open circles). To improve statistic, for each set of data, 190 snapshots were used. (B,C) Polarization of the complex. Δq is obtained as an integral of the absolute value of $\Delta\rho$ on a sphere of a certain radius r_{cut}. (B) Correlation between K^+–O distance and Δq(O), where O is an oxygen atom either belonging to carbonyl groups (circles) or water molecules (solid triangles). r_{cut} is taken equal to the C=O bond length (1.23 Å) [39]. Carbonyl oxygens of frame f5 are represented by solid circles. The inset plots the curves fitting the data. Use of different integration radii in the range 0–1.23 Å does not affect the plot at the qualitative level. (C) Induced charge of the complex around the K^+ ion contoured as a function of the frame number and of the cutoff integration radius r_{cut}.

(5–6 Å) and that these are more significant for carbonyl groups than for water. Thus, we conclude that, as expected, the carbonyl oxygens are more polarizable than the water molecules and that polarization increased when the number of ligands decreased (Fig. 2C,D).

As the charge difference induced by K^+ ion on the complex ΔQ depends crucially on the integration radius (r_{cut}), a plot of ΔQ as a function of r_{cut} and the frame number is of interest (Fig. 3C). The figure shows that initial (f0) and final (f10) ground states exhibited a similar ΔQ. In particular, in both cases, ΔQ was maximum (≈ 0.7 electrons) for $r_{cut} \approx 3.7$ Å, that is the first minimum in r_{K^+-O}. At the TS, the maximum polarization was shifted to larger r_{cut} values. That is, the contribution of the second-shell ligands (Val76 and Tyr78) to the potassium chemistry became significant as shown already in our geometrical analysis above (Fig. 3A).

3.3. Electronic structure

The Wannier orbitals are obtained from the Kohn-Sham orbitals with a unitary transformation [32]. The centers of these orbitals represent chemical concepts such as a covalent bond and electron lone pair [32,33]. Here we focus on the centers of the oxygen donor atoms, which represent the two electron lone pairs (W in Fig. 4A). In particular, we are interested in the *displacement* of the centers (Fig. 4A) upon potassium binding to the protein [34]. Fig. 4B,C plots the average displacements both in terms of distance from the oxygen atoms $\Delta(d(O-W))$ and angle with the carbonyl group $\Delta(\angle(C-O-W))$. The displacement of Val76 oxygens' lone pairs increased significantly during the dynamics. Indeed, on passing from S1 to S2, K^+ exchanged Tyr78 carbonyl with that of Val76. Thus, $d(K^+-O(Val76))$ decreased (Fig. 2A) and, consequently, K^+ increasingly polarized Val78 oxygens' lone pairs. In contrast, the displacement of Tyr78 carbonyl oxygens' lone pair decreased: $d(K^+-O(Tyr78))$ decreased. At a certain stage of the dynamics, the metal ion did not polarize Tyr78 lone pairs, which therefore became insensitive to the ion presence (triangles). The displacement experienced in the radial direction (~ 0.005 Å) is about the half of the angular one (~ 0.01 Å), indicating that the carbonylic oxygens' lone pairs were more easily bent than stretched. The lone pairs of Gly77 oxygen did not change significantly during the dynamics, which is consistent with the fact that they always bind the cation.

4. Discussion

This study has provided a detailed description of the coordination chemistry of the potassium ion during the translocation process from binding site S1 to binding site S2 in the selectivity filter of the potassium channel.

The binding sites S1 and S2 provide antiprismatic octahedron coordination geometry to the potassium ion [3] (Fig. 2B). Recent crystallographic data at higher resolution of the KcsA channel confirmed that all K^+ ions within the binding sites have this coordination symmetry [35,36]. In this respect, it is interesting to note that, on the basis of a 2.0 Å resolution structure, Morais-Cabral et al. [35] suggested that the same coordination polyhedron is present in a fully hydrated K^+ ion detected in the water just outside the mouth of the channel. In the present study, the exchange ligand's reaction with K^+ on passing from S1 to S2 is accompanied by the binding of water molecule Wat2. In the TS (between the two binding sites, Fig. 2), the ion coordination polyhedron changes to pyramidate triangular prism and the coordination number lowers to about seven.

Quantum chemical models have been used to investigate polarization effects. Although these models are relatively small (Fig. 1), simple electrostatic calculations suggest that they provide a fairly good description of K^+/protein inter-

Fig. 4. Displacement of Wannier centers upon potassium binding. (A) The Wannier centers (W, black dots) visualize the backbone carbonyl oxygens' lone pairs; The displacement of the W centers upon K^+ binding to the protein are reported in terms of O–W distance (B) and of C–O–W angle (C). Data for Val76, Gly77 and Tyr78 are plotted as circles, squares and triangles, respectively.

actions (see Material and methods). The polarization due to the K^+ ion is remarkably significant on the oxygen ligands and it is stronger on the carbonyl group than on the water (Fig. 3B), as already noted previously [37]. The effect of the potassium binding on the protein oxygens is not limited to a polarization effect, but it also involves changes in electronic structure as revealed by analysis of the geometry of the Wannier Centers (Fig. 4).

We conclude that differences in protein and water polarization (perhaps combined with changes in ligand geometry on passing from binding site to the TS) could play a key role for ion transport. These effects cannot be captured in standard force field for biomolecules.

We may expect that, during its permeation through the selectivity filter, Na^+ polarizes its oxygen donor atoms to a larger extent than K^+, as it is 'harder' than K^+ [38]. This could be in turn associated to the different energetics of the translocation process. Furthermore, one can speculate that differences in polarization effects in the adducts with K^+ and Na^+ might play a role in ionic selectivity.

The challenge is now to investigate K^+ and Na^+ permeation and selectivity in the KcsA channel using QM/MM methods [20].

Acknowledgements

References

[1] B. Hille, Ionic Channels of Excitable Membranes, Sinauer Associates, Sunderland, MA, USA, 1992.
[2] L.Y. Jan, Y.N. Jan, Annu. Rev. Neurosci. 20 (1997) 91.
[3] D.A. Doyle, J.M. Cabral, R.A. Pfuetzner, A. Kuo, J.M. Gulbis, S.L. Cohen, B.T. Chait, R. MacKinnon, Science 280 (1998) 69.
[4] B. Roux, R. MacKinnon, Science 285 (1999) 100.
[5] L. Guidoni, V. Torre, P. Carloni, Biochemistry 38 (1999) 8599.
[6] I.H. Shrivastava, M.S. Sansom, Biophys. J. 78 (2000) 557.
[7] S. Berneche, B. Roux, Biophys. J. 78 (2000) 2900.
[8] L. Guidoni, V. Torre, P. Carloni, FEBS Lett. 477 (2000) 37.
[9] J. Aqvist, V. Luzhkov, Nature 404 (2000) 881.
[10] V.B. Luzhkov, J. Aqvist, Biochim. Biophys. Acta 1548 (2001) 194.
[11] P.C. Biggin, G.R. Smith, I. Shrivastava, S. Choe, M.S. Sansom, Biochim. Biophys. Acta 1510 (2001) 1.
[12] T.P. Straatsma, H.J.C. Berendsen, J. Chem. Phys. 89 (1988) 5876.
[13] J. Aqvist, J. Phys. Chem. 94 (1990) 8021.
[14] B. Roux, Biophys. J. 71 (1996) 3177.
[15] G.O. Spessard, G.L. Miessler, Organometallic Chemistry, Prentice-Hall, Upper Saddle River, NJ, USA, 1997.
[16] F. Alber, O. Kuonen, L. Scapozza, G. Folkers, P. Carloni, Proteins 31 (1998) 453.
[17] H. Minoux, C. Chipot, J. Am. Chem. Soc. 121 (1999) 10366.
[18] J.W. Caldwell, P.A. Kollman, J. Am. Chem. Soc. 117 (1995) 4177.
[19] R. Car, M. Parrinello, Phys. Rev. Lett. 55 (1985) 2471.
[20] A. Laio, J. VandeVodele, U. Rothlisberger, J. Phys. Chem. (2002) in press.
[21] B. Roux, Chem. Phys. Lett. 212 (1993) 231.
[22] G. Nadig, L.C. van Zant, S.L. Dixon, K.M. Merz, J. Am. Chem. Soc. 120 (1998) 5593.
[23] M. Sulpizi, P. Schelling, G. Folkers, P. Carloni, L. Scapozza, J. Biol. Chem. 276 (2001) 21692.
[24] P. Hohenberg, W. Kohn, Phys. Rev. 136 (1964) B864–B871.
[25] W. Kohn, L.J. Sham, Phys. Rev. 140 (1965) A1133–A1138.
[26] A.D. Becke, Phys. Rev. A 38 (1988) 3098.
[27] C.L. Lee, W. Yang, R.G. Parr, Phys. Rev. B 37 (1988) 785.
[28] N. Troullier, J.L. Martins, Phys. Rev. B 43 (1991) 1993.
[29] R.N. Barnett, U. Landman, Phys. Rev. B 48 (1993) 2081.
[30] M.P. Allen, D.J. Tildesley, Computer Simulation of Liquids, Oxford Univ. Press, New York, 1987.
[31] H.L. Song, C.R. Jayendran, J. Phys. Chem. 100 (1996) 1420.
[32] N. Marzari, D. Vanderbilt, Phys. Rev. B 56 (1997) 12847.
[33] P.L. Silvestrelli, N. Marzari, D. Vanderbilt, M. Parrinello, Solid State Commun. 107 (1998) 7.
[34] S. Piana, P. Carloni, Proteins 39 (2000) 26.
[35] J.H. Morais-Cabral, Y. Zhou, R. MacKinnon, Nature 414 (2001) 37.
[36] Y. Zhou, J.H. Morais-Cabral, A. Kaufman, R. MacKinnon, Nature 414 (2001) 43.
[37] B. Roux, J. Comp. Chem. 16 (1995) 690.
[38] F.A. Cotton, G. Wilkinson, Advanced Inorganic Chemistry, Wiley, New York, 1988.
[39] S.J. Weiner, P.A. Kollman, D.T. Nguyen, D.A. Case, J. Comp. Chem. 7 (1986) 230.